

A miniature EEG node for synchronized wireless EEG sensor networks. [†]

Mathieu Baijot ¹, Abhijith Mundanad Narayanan ², Maria Brites Atalaia Rosa ¹, Jonathan Dan ^{2,3}, Alexander Bertrand ² and Michael Kraft ^{1,*}

¹ MNS, Department of Electrical Engineering (ESAT), University of Leuven, 3001 Leuven, Belgium

² STADIUS, Department of Electrical Engineering (ESAT), University of Leuven, 3001 Leuven, Belgium

³ Byteflies, 2600 Antwerp, Belgium

* Correspondence: michael.kraft@kuleuven.be

[†] Presented at 8th International Electronic Conference on Sensors and Applications, 1–15 November 2021;

Available online: <https://ecsa-8.sciforum.net>.

Abstract: The ability to record brain signals during daily life activities would allow to deepen our understanding of the human brain, its related pathologies (such as epilepsy and Alzheimer's disease) or develop practical and discreet brain-computer interfaces. In this paper, we present a new miniature wearable electroencephalography (EEG) sensor, of which multiple copies can be deployed on the scalp in a wireless mesh configuration to record brain activity. Each node in this wireless EEG sensor network (WESN) performs a local EEG acquisition which is transmitted via Bluetooth low energy to a smartphone. To keep coherent signals over time and avoid drifting, the nodes exchange synchronization pulses within the WESN via human body communication.

Keywords: EEG; wearable; epilepsy; seizure; HBC

1. Introduction

With the advent of wearable electronics, the ability to record physiological signals on the human body has grown. This is particularly the case for the human brain [1] where wearable technology could improve our understanding of brain pathologies (epilepsy, Alzheimer's diseases, etc.), or facilitate the use of brain-computer interfaces in daily life (e.g. for driver vigilance [2], neuro-steered hearing aids [3], etc.). Surface electroencephalography (EEG), where electrodes are placed on the scalp, has shown to be the most promising non-invasive solution for continuous monitoring of the brain 24/7 during daily life [4]. Multiple teams have already contributed to the development of wearable EEG systems such as [2,5–10]. While traditional EEG headsets are too bulky for use in real life, miniature EEG sensors come with their own disadvantage: they only cover a small region of the scalp (typically in or around the ears and on the forehead)[7–10]. In order to increase scalp coverage, while preserving wearability constraints, it was proposed in [4] to deploy multiple wireless miniature EEG sensors, this was dubbed a 'wireless EEG sensor network (WESN)' [4]. A first hardware prototype of this WESN concept has been proposed in [11]. In this paper, we focus on developing a wireless sensor that can be used as one node of an EEG sensor network. The sensor is designed to be as small as possible (24 mm × 7 mm × 3.6 mm) in order to be light and discrete enough to reduce its social impact and to stay as comfortable as possible. Furthermore, in order to synchronize the different nodes, we propose the use of synchronization pulses through human-body communication.

Citation: Lastname, F.; Lastname, F.; Lastname, F. Title. *Eng. Proc.* **2021**, *3*, x. <https://doi.org/10.3390/xxxxx>

Published: date

Publisher's Note: MDPI stays neutral with regard to jurisdictional claims in published maps and institutional affiliations.



Copyright: © 2021 by the authors. Submitted for possible open access publication under the terms and conditions of the Creative Commons Attribution (CC BY) license (<https://creativecommons.org/licenses/by/4.0/>).

2. Materials and Methods

The complete system consists of a group of wireless nodes connected to the scalp. Each node is composed of an EEG sensor, a wireless communication system, a central controlling unit, and a battery.

2.1. Surface EEG Sensor

The EEG circuit is intended to acquire and preprocess the brain activity measured on the scalp before being digitized via the 10-bit ADC of the central controlling unit. It is connected to three electrodes and is composed of three subparts that are described in this subsection.

The first step is to amplify the signal. This is done with an instrumentation amplifier configured with a gain of 26. A passive first-order high pass filter with a cut-off frequency of 0.3 Hz is then added to remove any DC component that would induce saturation during the next stage. Finally, a first-order low pass filter with a gain of 48 and a cut-off frequency of 250 Hz is used. Figure 1 shows a summary of the EEG sensor with a block diagram.

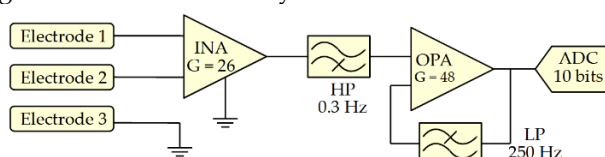


Figure 1. Block diagram of the EEG sensor.

2.2. Central Unit

The central controlling unit is implemented with the DA1453 chip[14] from Dialog Semiconductor. It contains, among others, a microcontroller and the complete required hardware to be compatible with Bluetooth low energy (BLE) 5.1. The central unit samples the EEG signal with its 10-bit ADC every 2 ms (500 Hz), concatenates them over time and sends them via BLE to a smartphone every 100 ms.

2.3 Synchronization

One problem when dealing with multiple autonomous nodes in a mesh system such as a WESN is that they all have their independent clock system. Every clock is designed to work at a specific frequency but has a small tolerance (usually +/- 10 ppm). Moreover, the frequency can vary over time, which results in a time-varying drift between the clocks. To overcome this problem, it was decided to send a synchronization pulse to each sensor by using the body as an electrical conductor. This is also known as galvanic Human Body Communication (HBC) or Body Channel Communication (BCC). As explained by Jang et al.[15], this consists of applying a voltage between two points on the body and measuring the induced voltage between two other independent points on the body. While HBC is usually used to transmit data, we used it to send a synchronization rectangular pulse. One node in the mesh is designed to be the master, the one sending the synchronization pulse; the remaining ones are designed to be the slaves, receiving the pulse.

To send the pulse, we used a general-purpose input/output (GPIO) pin of the microcontroller to send a rectangular pulse of 2 μ s every 250 ms. For the reception side, two active high pass filters with gains of 47 V/V and 10 V/V and a cut-off frequency of 6 kHz put in cascade are used to amplify the signal and maximally reduce the predominant 50 Hz noise and the biosignal. A Schmidt trigger is then used to recreate the initial pulse signal which is transmitted to a GPIO of the receiver. Figure 2 shows the block diagram of the receiver circuit.

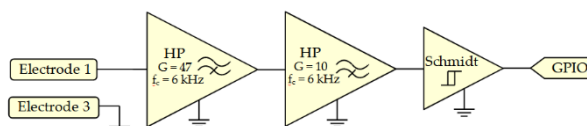


Figure 2. Block diagram of the synchronization receiver (RX).

The peaks captured by the nodes are then concatenated with the digitized EEG data and sent to the Bluetooth stream. To transmit and receive the synchronization pulse, the circuit uses the same electrodes as the one for EEG acquisition. Indeed, the bandwidth of both signals (EEG and synchronization pulse) are so far from each other that the input filter of the EEG can easily get rid of the synchronization signal (and vice versa).

2.4. Wireless communication

To transmit data via Bluetooth Low Energy 5.1., a service containing a single characteristic has been created. The choice to concatenate the EEG data with the synchronization bit (triggered by the HBC pulse as explained in Section 2.3) was made to reduce transmission packet size. A typical packet transmission is shown in Figure 3.

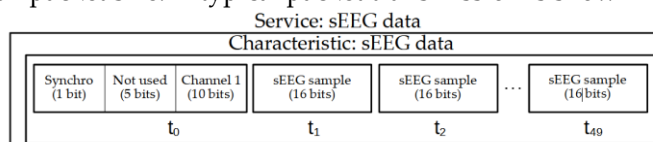


Figure 3. Each Bluetooth low energy packet transmitted contains 50 blocks concatenated. Each block of data contains synchronization information and the 10-bits EEG data.

2.5. Sensor fabrication

The three tests explained in the next section have been realized using a standard FR4 prototype PCB (Figure 4a). The final sensor, currently being developed, is shown in Figure 4b. To have the smallest possible sensor, flexible PCBs made of polyimide material of only 50 μm in thickness are used, leading to a maximal thickness of 1 mm with components included. The sensor uses two hearing aid A10 (Zinc-air) batteries connected in series. Since these batteries are 3.6 mm thick, the flexible PCB will be folded on itself to reduce its surface while not exceeding the thickness of the batteries.

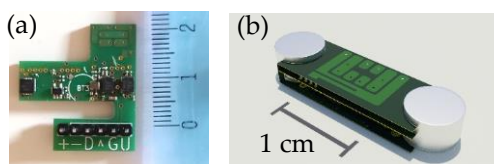


Figure 4. Design of one sensor node without electrodes: (a) current prototype PCB (b) CAD of the final sensor with folded PCB measuring 24 mm x 7 mm (with 3.6 mm thickness).

3. Results

3.1. EEG acquisition

The EEG acquisition was tested on its own and compared to a commercial mobile EEG device (SMARTING mobi from mbraintrain[12]), referred to as the reference system, in three different tests. During each test, silver chloride (AgCl) plastic cup electrodes were placed on the scalp of a test subject (29-year-old male) and connected to the sensor developed in this work as well as to the reference system using an electrode splitter.

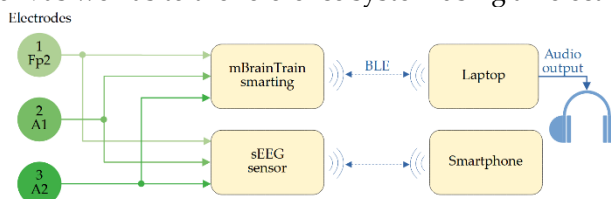


Figure 5. Test setup of the EEG acquisition system validation.

During the first test, the test subject is not asked to do anything special. Figure 6a shows the time signal acquired by this sensor and the reference system. Since both signals

have different gains, the two curves have been scaled and shifted vertically for better visibility. Figure 6b shows the computed cross-correlation of the two signals.

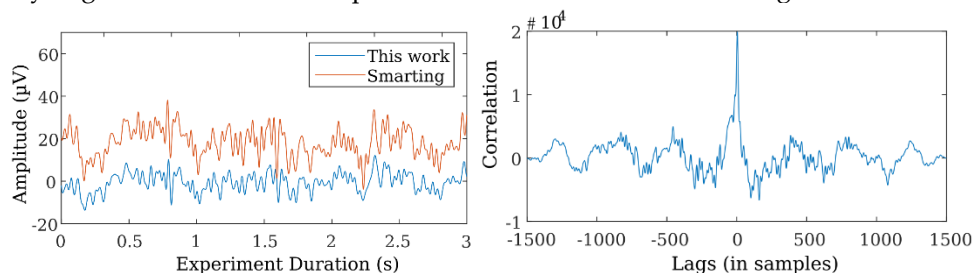


Figure 6. (a) The time-domain EEG signals (b) Cross-correlation of the two complete signals.

During the second test, the test subject is asked to keep his eyes open for one minute, then to close them for one minute. In this test, we expect to see alpha waves which are macroscopic neural oscillations in the range from 8 Hz to 12 Hz that appear when a test subject closes his eyes. Figure 7 shows the spectrum (discrete Fourier transform) of the EEG signals acquired by both devices: the first minutes of the test (eyes open, Figure 7a) and the second minute of the test (eyes closed, Figure 7b).

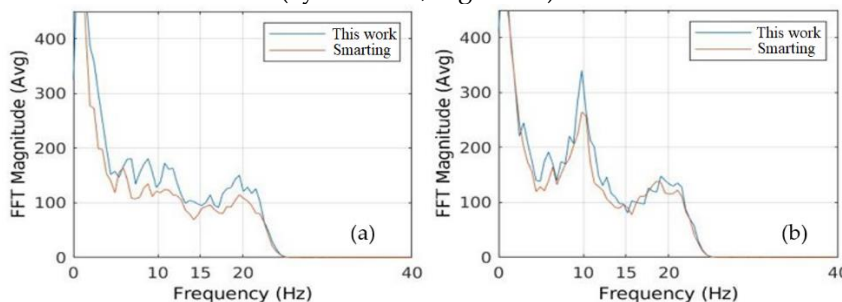


Figure 7. Capture of alpha waves. Both signals have been post-processed to remove any frequency higher than 25 Hz. (a) Spectrum of the EEG signal when test subject kept eyes open. (b) Spectrum of the EEG signal when test subject kept eyes closed.

During the third test, called “oddball”, the test subject is asked to listen to a stream of short sounds (“bip”) at 600 Hz played every second (called background). Randomly and seldomly, the standard tone is replaced by a higher pitch tone at 900 Hz (called target). The test subject must then count the number of higher tones heard during the total test (12 minutes). These random target tones elicit a so-called event-related potential (ERP), which typically appears 300 ms after the stimulus (the so-called ‘P300’ response). To process the data, every 1 s window following a bip is sorted based on its tone. Higher and lower tone event windows are averaged separately and compared. It is expected to see a variation in the brain activity when a higher tone is heard due to the ERP. Figure 8 shows the results.

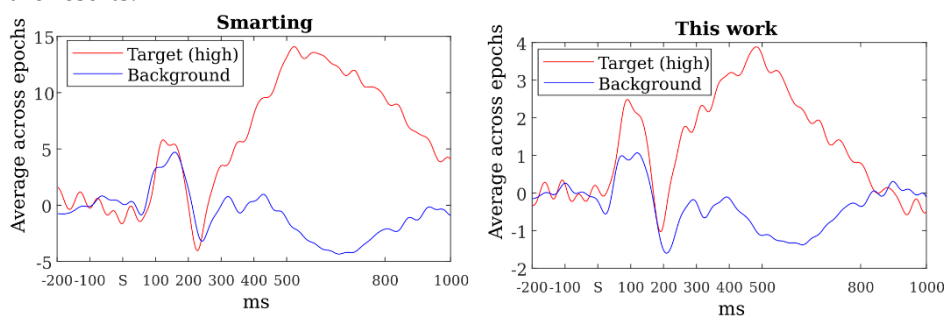


Figure 8. Responses to the target tone versus standard (background) tone in the oddball test. (a) Result from the reference system. (b) Result from the sensor system developed in this work.

3.2. Synchronization

This part of the project has not been tested in a full configuration while recording EEG. It has been tested on its own as early validation. Two nodes were connected to the body (arm) via two electrodes as shown in Figure 9. The first node was the emitter (TX), sending a $2\ \mu\text{s}$ rectangular pulse using a GPIO pin, and the second node was the receiver (RX), receiving the pulse reconstructed after amplification and filtering, via one GPIO pin.

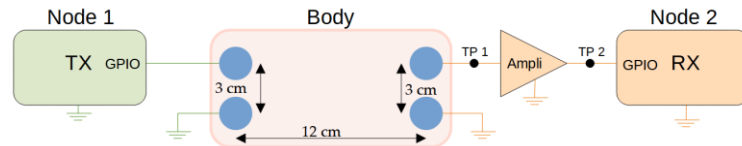


Figure 9. Test setup of the HBC validation test. Note that the green ground and orange ground are not connected. Test points TP1 and TP2 are used to visualize steps on the reception side (see Figure 10).

Figure 10c shows the output of the signal where the internal state of the microcontroller changes after each synchronization pulse being received. Figure 10a shows the signal measured before amplification and filtering and Figure 10b shows the signal sent to the microcontroller (after the two amplification stages and the Schmitt trigger).

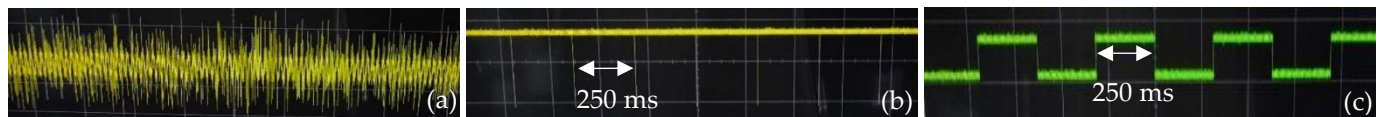


Figure 10. the signal received and processed by the synchronization receiver. (a) The measured signal on the electrodes before any amplification (on TP1). (b) Processed signal (after the two stages amplification and the Schmitt trigger, measured on TP2). (c) The internal state of the microcontroller which toggles every time a synchronization pulse is received.

4. Discussion

4.1. EEG acquisition

During the first test, we could validate the ability of the sensor system to provide similar output as a commercial device. Figure 6a shows that the time-domain signals look similar. This first observation was then confirmed by the cross-correlation of the two signals, which has a clear dominant peak around 0 lags in Figure 6b.

The second test was also successfully passed. Alpha waves were expected between 8 and 12 Hz when the test subject had his eyes closed. In Figure 7b, a clear peak rose around 10 Hz as expected when the subject closed his eyes while none were visible when his eyes were open. Moreover, similar phenomena were observed in the reference system.

Results from the third test are more complex to analyze. Standard oddball curves might strongly vary depending on the test subject, electrodes positions, synchronization between EEG and audio, ... We can however validate a few points in Figure 8 showing that the test was successfully passed. First, the typical peak around 100 ms, showing a brain reaction when the subject heard a sound, is present. Furthermore, we observe a clear difference between the background and target curve, because of the ERP.

4.2. Synchronization

The use of HBC as synchronization has shown promising results. While the signal measured at the skin level is highly corrupted by 50Hz noise, proper filtering allows recovering the initial synchronization pulses. A further study will be required to estimate the number of pulses missed (or artificial detections) on the receiver side compared to the emitter side.

Author Contributions:

Conceptualization, M.B., M.R. and A.B.; methodology, M.B., A.M.N. and J.D.; software, M.B. and A.M.N.; validation, M.B., M.R., A.M.N. and J.D.; formal analysis, A.M.N.; writing—original draft preparation, M.B.; writing—review and editing, J.D., A.B. and M.K.; supervision, A.B. and M.K.; funding acquisition, A.B. All authors have read and agreed to the published version of the manuscript.”

Funding: This work has received funding from the European Research Council (ERC) under the European Union’s Horizon 2020 research and innovation program (grant agreement no. 802895).

Informed Consent Statement: Informed consent was obtained from all subjects involved in the study.

Conflicts of Interest: The authors declare no conflict of interest. The funders had no role in the design of the study; in the collection, analyses, or interpretation of data; in the writing of the manuscript, or in the decision to publish the results.

References

1. Casson, A.J. Wearable EEG and Beyond. *Biomed. Eng. Lett.* **2019**, *9*, 53–71, doi:10.1007/s13534-018-00093-6. 14
2. Chin-Teng Lin; Chun-Hsiang Chuang; Chih-Sheng Huang; Shu-Fang Tsai; Shao-Wei Lu; Yen-Hsuan Chen; Li-Wei Ko Wireless and Wearable EEG System for Evaluating Driver Vigilance. *IEEE Trans. Biomed. Circuits Syst.* **2014**, *8*, 165–176, doi:10.1109/TBCAS.2014.2316224. 15
3. Van Eyndhoven, S.; Francart, T.; Bertrand, A. EEG-Informed Attended Speaker Extraction From Recorded Speech Mixtures With Application in Neuro-Steered Hearing Protheses. *IEEE Trans. Biomed. Eng.* **2017**, *64*, 1045–1056, doi:10.1109/TBME.2016.2587382. 16
4. Bertrand, A. Distributed Signal Processing for Wireless EEG Sensor Networks. *IEEE Trans. Neural Syst. Rehabil. Eng.* **2015**, *23*, 923–935, doi:10.1109/TNSRE.2015.2418351. 17
5. Zhang, X.; Li, J.; Liu, Y.; Zhang, Z.; Wang, Z.; Luo, D.; Zhou, X.; Zhu, M.; Salman, W.; Hu, G.; et al. Design of a Fatigue Detection System for High-Speed Trains Based on Driver Vigilance Using a Wireless Wearable EEG. *Sensors* **2017**, *17*, 486, doi:10.3390/s17030486. 18
6. Byteflies NV Byteflies Available online: <https://www.byteflies.com/> (accessed on 9 August 2021). 19
7. Athavipach; Pan-ngum; Israsena A Wearable In-Ear EEG Device for Emotion Monitoring. *Sensors* **2019**, *19*, 4014, doi:10.3390/s19184014. 20
8. Zhang, R.; Bernhart, S.; Amft, O. Diet Eyeglasses: Recognising Food Chewing Using EMG and Smart Eyeglasses. In Proceedings of the 2016 IEEE 13th International Conference on Wearable and Implantable Body Sensor Networks (BSN); IEEE: San Francisco, CA, USA, June 2016; pp. 7–12. 21
9. Epitel Epitel Inc | Epilepsy Monitoring + Control | Salt Lake City Available online: <https://www.epitel.com/>. 22
10. Sopic, D.; Aminifar, A.; Atienza, D. E-Glass: A Wearable System for Real-Time Detection of Epileptic Seizures. In Proceedings of the 2018 IEEE International Symposium on Circuits and Systems (ISCAS); IEEE: Florence, 2018; pp. 1–5. 23
11. Tang, T.; Yan, L.; Park, J.H.; Wu, H.; Zhang, L.; Lee, H.Y.B.; Yoo, J. 34.6 EEG Dust: A BCC-Based Wireless Concurrent Recording/Transmitting Concentric Electrode. In Proceedings of the 2020 IEEE International Solid-State Circuits Conference - (ISSCC); IEEE: San Francisco, CA, USA, February 2020; pp. 516–518. 24
12. World Health Organization (WHO) Epilepsy Available online: <https://www.who.int/news-room/fact-sheets/detail/epilepsy> (accessed on 9 August 2021). 25
13. Devinsky, O.; Spruill, T.; Thurman, D.; Friedman, D. Recognizing and Preventing Epilepsy-Related Mortality: A Call for Action. *Neurology* **2016**, *86*, 779–786, doi:10.1212/WNL.0000000000002253. 26
14. Ultra Low Power Bluetooth 5.1 SoC Available online: https://www.dialog-semiconductor.com/sites/default/files/2021-03/DA14531_datasheet_3v3_0.pdf. 27
15. Jang, J.; Bae, J.; Yoo, H.-J. Understanding Body Channel Communication: A Review: From History to the Future Applications. In Proceedings of the 2019 IEEE Custom Integrated Circuits Conference (CICC); IEEE: Austin, TX, USA, April 2019; pp. 1–8. 28